

Normalization of Skeletal Muscle Glycogen Synthesis and Glycolysis in Rosiglitazone-Treated Zucker Fatty Rats

An In Vivo Nuclear Magnetic Resonance Study

Beat M. Jucker,¹ Thomas R. Schaeffer,² Robin E. Haimbach,² Thomas S. McIntosh,³ Daniel Chun,⁴ Matthew Mayer,¹ Derek H. Ohlstein,¹ Hugh M. Davis,³ Stephen A. Smith,⁵ Alexander R. Cobitz,⁵ and Susanta K. Sarkar⁶

The aim of this study was to characterize insulin-stimulated skeletal muscle glucose metabolism in Zucker fatty rats and to provide insight into the therapeutic mechanism by which rosiglitazone increases insulin-stimulated glucose disposal in these rats. Metabolic parameters were measured using combined in vivo ¹³C nuclear magnetic resonance (NMR) spectroscopy to measure skeletal muscle glucose uptake and its distributed fluxes (glycogen synthesis and glycolysis), and ³¹P NMR was used to measure simultaneous changes in glucose-6-phosphate (G-6-P) during a euglycemic-hyperinsulinemic clamp in awake Zucker fatty rats. Three groups of Zucker fatty rats (fatty rosiglitazone [FRSG], fatty control [FC], lean control [LC]) were treated for 7 days before the experiment (3 mg/kg rosiglitazone or vehicle via oral gavage). Rates of glycolysis and glycogen synthesis were assessed after treatment by monitoring 1,6-¹³C₂ glucose label incorporation into 1-¹³C glycogen, 3-¹³C lactate, and 3-¹³C alanine during a euglycemic (~7–8 mmol/l)-hyperinsulinemic (10 mU · kg⁻¹ · min⁻¹) clamp. The FRSG group exhibited a significant increase in insulin sensitivity, reflected by an increased whole-body glucose disposal rate during the clamp (24.4 ± 1.9 vs. 17.6 ± 1.4 and 33.2 ± 2.0 mg · kg⁻¹ · min⁻¹ in FRSG vs. FC [*P* < 0.05] and LC [*P* < 0.01] groups, respectively). The increased insulin-stimulated glucose disposal in the FRSG group was associated with a normalization of the glycolytic flux (52.9 ± 9.1) to LC (56.2 ± 16.6) versus FC (18.8 ± 8.6 nmol · g⁻¹ · min⁻¹, *P* < 0.02) and glycogen synthesis flux (56.3 ± 11.5) to LC (75.2 ± 15.3) versus FC (16.6 ± 12.8 nmol · g⁻¹ ·

min⁻¹, *P* < 0.05). [G-6-P] increased in the FRSG and LC groups versus baseline during the clamp (13.0 ± 11.1 and 16.9 ± 5.8%, respectively), whereas [G-6-P] in the FC group decreased (-23.3 ± 13.4%, *P* < 0.05). There were no differences between groups in intramyocellular glucose, as measured by biochemical assay. These data suggest that the increased insulin-stimulated glucose disposal in muscle after rosiglitazone treatment can be attributed to a normalization of glucose transport and metabolism. *Diabetes* 51:2066–2073, 2002

Rosiglitazone, a member of the thiazolidinedione (TZD) class of oral antihyperglycemic agents used to treat type 2 diabetes, is a potent peroxisome proliferator-activated receptor (PPAR)- γ agonist. Studies in animal models of type 2 diabetes show that rosiglitazone improves glycemic control by enhancing insulin-stimulated whole-body glucose disposal (1,2). The increase in whole-body insulin sensitivity is the result of increased insulin action in skeletal muscle (1,3,4), liver (1,4), and adipose tissue (5,6). Skeletal muscle accounts for the largest proportion of insulin-stimulated whole-body glucose uptake (7); therefore, much of the focus on the insulin-sensitizing benefits of TZDs has been targeted to this tissue (1,3,4,8–12). Although skeletal muscle expresses low levels of PPAR- γ (13) and direct actions of TZDs on muscle glucose metabolism in vitro have been reported (5,9,14), the precise mechanism of action of TZDs in skeletal muscle is unclear. Much evidence exists to suggest that the improvement in muscle insulin sensitivity may be an indirect consequence of activation of PPAR- γ in fat, a tissue in which the receptor is abundantly expressed. Activation of PPAR- γ in fat results in decreased adipocyte lipolysis and hence free fatty acid availability (1,2,4,15). This in turn would lead to a subsequent decrease in intramyocellular lipid content (4). A number of recent clinical studies have demonstrated the direct correlation between intramyocellular lipid content and insulin sensitivity (16–18). It is also well established that an increase in plasma free fatty acids results in decreased insulin-stimulated glucose uptake in skeletal muscle via an inhibition of the insulin-signaling cascade (19,20) and/or inhibition of

From ¹Cardiovascular and Urogenital Investigational Biology and Product Support, GlaxoSmithKline, King of Prussia, Pennsylvania; the ²Laboratory of Animal Sciences, GlaxoSmithKline, King of Prussia, Pennsylvania; ³Clinical Pharmacology, GlaxoSmithKline, King of Prussia, Pennsylvania; ⁴Musculoskeletal Diseases, GlaxoSmithKline, King of Prussia, Pennsylvania; ⁵Clinical Development, GlaxoSmithKline, King of Prussia, Pennsylvania; and ⁶Technology Development, GlaxoSmithKline, King of Prussia, Pennsylvania.

Address correspondence and reprint requests to Dr. Beat M. Jucker, GlaxoSmithKline, UW2940, 709 Swedeland Rd., King of Prussia, PA 19406. E-mail: beat_m_jucker@gsk.com.

Received for publication 21 November 2001 and accepted in revised form 9 April 2002.

APE, atom percent excess; EGP, endogenous glucose production; FC, fatty control; FRSG, fatty rosiglitazone; G-6-P, glucose-6-phosphate; GDR, glucose disposal rate; G_{inf} , glucose infusion rate; LC, lean control; NMR, nuclear magnetic resonance; PCr, phosphocreatine; PPAR, peroxisome proliferator-activated receptor; TZD, thiazolidinedione; V_{gly} , glycolytic flux; V_{glyc} , glycogen synthesis rate.

glycolysis through substrate competition (glucose–fatty acid cycle) (21).

However, a comprehensive analysis of the effects of TZDs on muscle glucose uptake and its subsequent metabolism in vivo has not been performed. The purpose of the present study was to use a combination of in vivo ^{13}C and ^{31}P nuclear magnetic resonance (NMR) noninvasive spectroscopic techniques to simultaneously measure skeletal muscle glucose uptake, glycogen synthesis, glycolysis, and glucose-6-phosphate (G-6-P) under euglycemic-hyperinsulinemic clamp conditions in conscious Zucker fatty rats following rosiglitazone treatment.

RESEARCH DESIGN AND METHODS

Animals. Zucker obese (*fa/fa*) rats and their lean littermates (Harlan, Indianapolis, IN) were housed in an environmentally controlled room with a 12-h light/dark cycle. Obese and nonobese rats (8–10 weeks old) were placed on a pair-fed diet (#5L35; LabDiet, Richmond, IN) consisting of 100 kcal/day for 5–10 days before surgery. Rats were chronically catheterized (carotid artery and jugular vein) as described elsewhere (22), and the feeding regimen was continued for an additional 7 days. Rats were placed into three groups: fatty rosiglitazone (FRSG) ($n = 12$), fatty control (FC) ($n = 9$), and lean control (LC) ($n = 8$). Immediately upon completion of the surgical procedure, rats were begun on a 7-day drug treatment protocol. The FRSG group received 3 mg/kg rosiglitazone (rosiglitazone maleate) via oral gavage once daily, and the control groups received vehicle (sterile water). Catheters were kept patent by flushing 1–3 days before the infusion experiment.

In vivo experiments. All rats were fasted overnight before the infusion experiment. Rats were acclimated to restraint by being positioned in restraining tubes for 1 and 2 h, respectively, in the 2 days before the experiment. On the day of the experiment, rats were placed into a customized restraining tube that allowed their left hindlimb to be secured to the outside of the tube in a manner to limit free movement of the leg for NMR measurements. The rats were transiently anesthetized (<30 s) with 2.0% isoflurane (Abbott Laboratories, Chicago) so they could be placed in the restraining tube. A euglycemic-hyperinsulinemic ($10 \text{ mU} \cdot \text{kg}^{-1} \cdot \text{min}^{-1}$ Humulin Regular; Eli Lilly, Indianapolis, IN) clamp was begun using 1,6- $^{13}\text{C}_2$ glucose (99% enriched, 20% wt/vol; Cambridge Isotope Laboratories, Cambridge, MA) at 2.5 min after the commencement of the primed continuous insulin infusion. Plasma glucose concentrations were clamped between 7 and 8 mmol/l. All clamps lasted for 150 min. Blood samples were drawn during the baseline NMR measurement, at 7.5 min, 15 min, and every 15 min thereafter for immediate assessment of plasma glucose and lactate concentrations. At the end of the in vivo NMR experiment, rats were anesthetized with an intravenous dose of 50 mg/kg Nembutal (Abbott Laboratories). Superficial skin was rapidly removed from the left hindquarter followed by in situ freeze clamping of the gastrocnemius and biceps femoris muscles. Rats were killed with a lethal dose of Nembutal.

In vivo NMR spectroscopy. All in vivo ^{13}C and ^{31}P NMR experiments were performed on a Bruker ABX system (horizontal/40-cm diameter bore, 4.7-Tesla field strength magnet; Bruker Medical, Billerica, MA). Both ^{13}C observe/ ^1H decouple and ^{31}P observe NMR spectroscopy were performed using a triple tune radio frequency probe consisting of concentric surface coils (the outer ^1H coil [42 mm] tuned to 200.21 MHz, and the inner dual frequency ^{13}C or ^{31}P coil [25 mm] tuned to 50.34 and 81.05 MHz, respectively). The rat hindlimb was positioned over the $^{13}\text{C}/^{31}\text{P}$ coil (vertical in plane) and placed in the magnet isocenter. Because of the intrinsic low $^{13}\text{C}/^{31}\text{P}$ sensitivity in the hindlimb experiments, it was necessary to measure the bulk signal from the larger tissue beds of mixed fiber type including the gastrocnemius and biceps femoris. ^1H decoupled- ^{13}C NMR spectroscopy was performed in the following manner: an initial frequency selective sinc pulse (20 ms) set on the low-field side of the methylene carbon of lipids at 30 ppm was immediately followed by a nonselective hard pulse ($\sim 70^\circ$ flip angle, 7 mm from surface coil). The sinc pulse power was adjusted to eliminate most of the signals in that region. Broadband ^1H Waltz-8 decoupling was applied during acquisition, and additional Nuclear Overhauser Enhancement was achieved using low-power decoupling during the relaxation delay (TR = 0.5 s, SW = 10 KHz, 2 K data). A 15-min baseline spectrum was followed by subsequent 15-min acquisitions throughout the duration of the experiment. ^{13}C NMR spectra were processed semiautomatically using a Gaussian filter and baseline flattening before peak integration (Nuts NMR processing software; Acorn NMR, Fremont, CA).

^{31}P NMR was performed using a hard pulse (45° flip angle) that was optimized 7 mm from the surface coil (TR = 1 s, SW = 3 KHz, 2 K data). Two 10-min spectra were acquired: one at baseline and the other at 140–150 min.

^{31}P NMR spectra were processed using Gaussian resolution enhancement. In all spectra, the phosphocreatine (PCr) peak was set to 0 ppm, and β -ATP and G-6-P peaks were integrated using Nuts NMR processing software (21). [G-6-P] was extrapolated from the in vivo spectra after correction for differential saturation with respect to the β -ATP peak and enzyme assay–derived ATP concentrations (modified diagnostic kit no. 366; Sigma, St. Louis, MO).

The creatine/PCr peak (54.4 ppm) in the ^{13}C spectrum and γ -ATP (–16.0 ppm) in the ^{31}P spectrum were used as an internal reference standard for movement of the leg. If severe movement compromised these peak integrals, the experiment was terminated.

Tissue extract analysis. Muscle tissue extracts were prepared for high-field NMR analysis by homogenizing ~ 0.5 g skeletal muscle as previously described (21). NMR analysis was performed at 9.4 Tesla (Bruker WB-400 AMX NMR spectrometer; Bruker). Proton-observed carbon-enhanced spectroscopy was performed on tissue extract samples for fractional enrichment calculations (21). For quantitation, a correction factor was calculated when a TR (pulse repetition time) equaling 30 s was used. Alanine concentration was quantitated by comparing its signal intensity with a known internal concentration standard (lactate), which was measured in tissue extracts using a 2300 STAT PLUS analyzer (Yellow Springs Instruments, Yellow Springs, OH).

Analytical procedures. Plasma glucose concentrations were measured using a 2300 STAT PLUS analyzer. Plasma immunoreactive free insulin was measured with a double-antibody radioimmunoassay technique (Linco Research, St. Charles, MO). The 1,6- $^{13}\text{C}_2$ enrichment of plasma glucose was determined using an LC/MS (liquid chromatography/mass spectrometry) system (Agilent Technologies LC/MSD 1100) (23). The MS electrospray chamber conditions were set for positive ionization. Selected ion monitoring was used to detect the sodium adducts (M^+23^+) of each glucose isotope, with a $m/z = 203$ ion corresponding to the sodium adduct of normal glucose and a $m/z = 205$ ion corresponding to the sodium adduct of 1,6- $^{13}\text{C}_2$ glucose. Standard curves were generated (0–97% 1,6- $^{13}\text{C}_2$ glucose atom percent excess [APE]). Plasma samples were extracted using ice-cold acetone, and 5 μl was injected into the column.

Glycogen 1,6- $^{13}\text{C}_2$ fractional enrichments were determined using the isolated glycogen after perchloric acid extraction (21), and absolute glycogen concentrations were measured using a separate portion of muscle as previously described (24). Intramyocellular glucose was calculated by measuring free glucose in the tissue extracts and correcting for extracellular space using an intra/extracellular space ratio of 9.0 and plasma glucose assumed to be equal to the extracellular space glucose (25). Plasma triglyceride concentrations were determined enzymatically using an Olympus AU600 analyzer (Olympus Optical, Melville, NY).

Endogenous glucose production calculation. Endogenous glucose production (EGP) was estimated by taking the difference of the glucose infusion rate (G_{inf}) and the tracer-determined whole-body glucose disposal rate (GDR). Whole-body GDR was calculated from G_{inf} and the steady-state plasma 1,6- $^{13}\text{C}_2$ glucose enrichment at 120 min.

Glycogen synthesis rate (V_{glyc}) calculation. The incremental change in C-1 glycogen peak intensity from 1,6- $^{13}\text{C}_2$ glucose incorporation was measured at 100.5 ppm. Incremental plasma glucose ^{13}C fractional enrichment as well as final glycogen ^{13}C enrichment and concentrations were used to back-extrapolate the glycogen concentration ($\mu\text{mol/g}$, which represents micromoles glucosyl units per gram muscle wet weight) at each measured time point to baseline, as described by Bloch et al. (26). Glycogen synthesis rates were determined using a linear regression analysis over the individual time point glycogen concentrations.

Glycolytic flux calculations. Metabolic steady-state conditions were assumed for calculating carbon flux through the glycolytic pathway into the intermediate triose pool of lactate, pyruvate, and alanine (Fig. 1).

Differential equations were developed from steady-state rate equations and solved for glycolytic flux (V_{gly}) (27). ^{13}C label incorporation from 1,6- $^{13}\text{C}_2$ glucose into 3- ^{13}C lactate and 3- ^{13}C alanine in the hindlimb muscles may be used as an indirect marker of pyruvate labeling. Therefore, the 3- ^{13}C lactate and 3- ^{13}C alanine turnover rate provides a qualitative index of V_{gly} . The absolute flux was calculated by simultaneously solving the differential equations describing the V_{gly} using CWave software (Dr. Graeme F. Mason, Yale University). The parameters required for the modeling of V_{gly} include plasma 1,6- $^{13}\text{C}_2$ glucose, tissue 3- ^{13}C lactate and 3- ^{13}C alanine turnover curves, and lactate and alanine concentrations. A limitation of this measurement is that the turnover of the plasma glucose pool must be faster than that of the lactate and alanine pools. Therefore, these measurements can only be made under hyperinsulinemic conditions when plasma glucose turnover is increased (27).

The traditional method by which skeletal muscle V_{gly} is measured in vivo is an indirect one. It is calculated as the difference between glucose uptake rates as assessed using the 2-deoxyglucose method and glycogen synthesis rate as

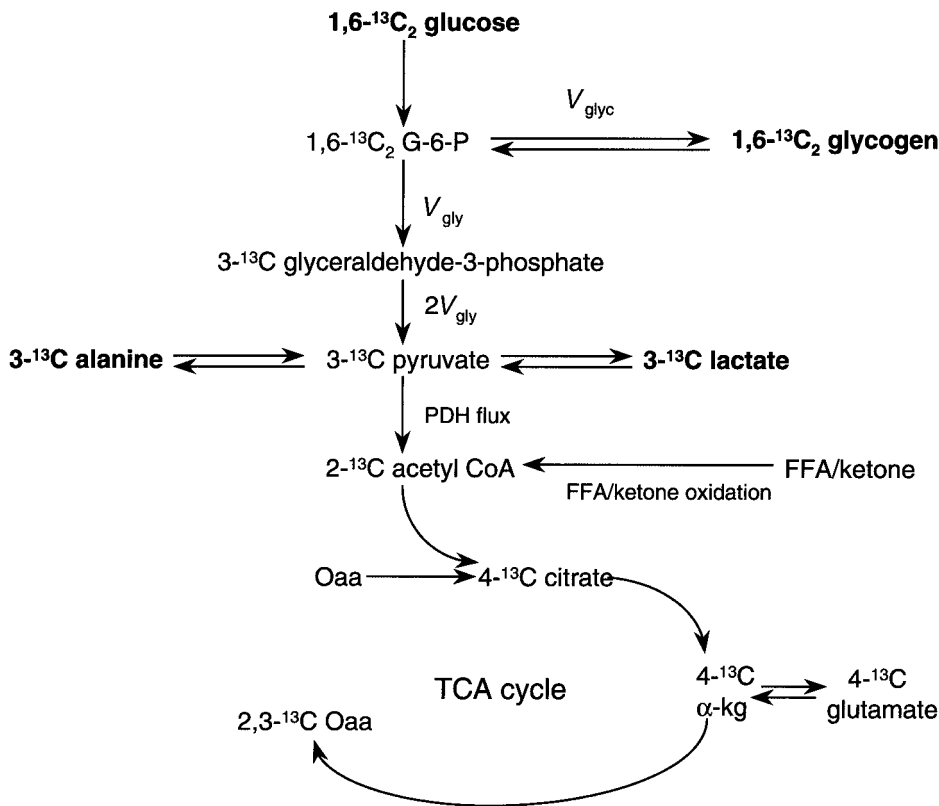


FIG. 1. Schematic of skeletal muscle metabolite labeling after 1,6-¹³C₂ glucose precursor infusion. ¹³C label from glucose becomes incorporated into 1,6-¹³C₂ glycogen and 3-¹³C pyruvate, which can be reduced to 3-¹³C lactate or converted to 3-¹³C alanine via aminotransferase reaction. The rate at which substrate enters the [lactate+pyruvate+alanine] pool is two times the glycolytic rate ($2V_{gly}$). The benefit of using the doubly labeled (1,6-¹³C₂) glucose precursor is to double the 3-¹³C enrichment in lactate and alanine. α -k-g, α -ketoglutarate; FFA, free fatty acid; Oaa, oxaloacetate; PDH, pyruvate dehydrogenase.

assessed using ³H or ¹⁴C glucose (28). Whole-body glycolysis may be calculated using the ³H glucose washout method (29).

Statistical analysis. All data are reported as means \pm SE. ANOVA was performed on data to determine the significance at a minimum threshold of $P < 0.05$ between the three groups. A multiple comparison Newman-Keuls post hoc test was used when necessary to determine significance between the groups.

RESULTS

Posttreatment baseline measurements. As a result of the pair-feeding protocol, there were no differences in weight between the FC (350 ± 4 g) and FRSG (345 ± 5 g) groups. However, both groups weighed significantly more than the LC group (291 ± 3 g, $P < 0.001$). The weight gain during the treatment period was 29 ± 3 , 30 ± 2 , and 11 ± 1 g in the FC, FRSG, and LC groups, respectively ($P < 0.001$ LC vs. FC and FRSG). Surprisingly, there were no differences in basal insulin concentrations between the FRSG (428 ± 77 pmol/l) and FC (475 ± 111 pmol/l) groups, but both groups had significantly higher concentrations than the LC group (125 ± 28 pmol/l, $P < 0.05$). Basal plasma glucose in the FRSG group (8.7 ± 0.6 mmol/l) was significantly reduced compared with that of the FC group (13.5 ± 0.8 mmol/l, $P < 0.001$) and was normalized to the LC group (7.5 ± 0.4 mmol/l). Basal plasma triglyceride concentration in the FRSG group (114 ± 12 mg/dl) was also lower than that in the FC group (273 ± 37 mg/dl, $P < 0.001$) but higher than that in the LC group (32 ± 3 mg/dl, $P < 0.01$).

Euglycemic-hyperinsulinemic clamp. During the euglycemic-hyperinsulinemic clamp experiment, plasma glucose concentrations were maintained at ~ 7 – 8 mmol/l (Table 1). Although steady-state insulin concentrations during the euglycemic-hyperinsulinemic clamp were similar in the FC and FRSG groups, they were significantly

higher than those in the LC group (Table 1). Glucose turnover was increased in the FRSG group after treatment. This may be visualized in Fig. 2 because the plasma 1,6-¹³C₂ glucose APE increased rapidly during the clamp in the LC and FRSG groups but was slower in the FC group. G_{inf} at 120 min was significantly higher in the FRSG group (20.3 ± 1.9 mg \cdot kg⁻¹ \cdot min⁻¹) than in the FC group (13.8 ± 1.4 mg \cdot kg⁻¹ \cdot min⁻¹, $P < 0.05$) but lower than in the LC group (30.1 ± 1.8 mg \cdot kg⁻¹ \cdot min⁻¹, $P < 0.01$; Table 1). EGP did not differ in the three groups; therefore, whole-body GDR was also higher in the FRSG group than in the FC group. However, whole-body GDR in the FRSG group was not normalized to the LC group (Table 1).

In vivo ¹³C NMR. Baseline subtracted ¹³C NMR spectra depicting ¹³C label turnover in a LC rat during a euglycemic-hyperinsulinemic clamp is shown in Fig. 3. The β and α anomer peaks of 1-¹³C glucose appear at 96.8 and 93.0 ppm, respectively, and the large peak slightly downfield at 100.5 ppm corresponds to the C-1 glucosyl unit of the glycogen polymer. The C-6 glucosyl unit of the glycogen polymer resides at 61.4 ppm and is significantly larger than C-1 because of the overlapping 6-¹³C peak. 3-¹³C lactate and 3-¹³C alanine may also be observed at 21.0 and 16.9 ppm, respectively. The absolute steady-state V_{glyc} was significantly reduced in the FC group (16.6 ± 12.8 nmol \cdot g⁻¹ \cdot min⁻¹) versus the LC group (75.2 ± 15.3 nmol \cdot g⁻¹ \cdot min⁻¹, $P < 0.05$) but was normalized in the FRSG group (56.3 ± 11.5 nmol \cdot g⁻¹ \cdot min⁻¹, $P < 0.05$ vs. FC, Table 1). The best-fit label turnover curves to 3-¹³C pyruvate are shown in Fig. 4. Empirically, the 3-¹³C pyruvate turnover in the LC and FRSG groups is more rapid than in the FC group. This increased label turnover in the LC and FRSG groups versus the FC group may be used as a qualitative

TABLE 1
Euglycemic-hyperinsulinemic clamp

Group	Plasma glucose (mmol/l)	Plasma insulin (pmol/l)	G_{inf} ($\text{mg} \cdot \text{kg}^{-1} \cdot \text{min}^{-1}$)	EGP ($\text{mg} \cdot \text{kg}^{-1} \cdot \text{min}^{-1}$)	Whole-body GDR ($\text{mg} \cdot \text{kg}^{-1} \cdot \text{min}^{-1}$)	V_{glyc} ($\text{nmol} \cdot \text{g}^{-1} \cdot \text{min}^{-1}$)	V_{gly} ($\text{nmol} \cdot \text{g}^{-1} \cdot \text{min}^{-1}$)
LC	6.7 ± 0.5	2045 ± 701 [†]	30.1 ± 1.8	3.7 ± 0.1	33.2 ± 2.0	75.2 ± 15.3 [†]	56.2 ± 16.6 [§]
FC	8.1 ± 0.4	5725 ± 1160	13.8 ± 1.4 [*]	3.8 ± 0.1	17.6 ± 1.4 [*]	16.6 ± 12.8	18.8 ± 8.6
FRSG	7.5 ± 0.4	3701 ± 672	20.3 ± 1.9 ^{†‡}	4.2 ± 0.5	24.4 ± 1.9 ^{†‡}	56.3 ± 11.5 [†]	52.9 ± 9.1 [§]

Data are means ± SE. Plasma glucose, G_{inf} , EGP, and whole-body GDR were calculated at 120 min after steady-state glucose turnover had been achieved. * $P < 0.001$ vs. LC; † $P < 0.05$ vs. FC; ‡ $P < 0.01$ vs. LC; § $P < 0.02$ vs. FC.

marker of increase flux through glycolysis in these groups (24). Absolute V_{gly} was calculated using the metabolic steady-state turnover kinetics of ^{13}C label in 3- ^{13}C lactate and 3- ^{13}C alanine pools. The benefit of using the doubly labeled (1,6- $^{13}\text{C}_2$) glucose precursor is to double the 3- ^{13}C enrichment in lactate and alanine, thereby providing greater NMR sensitivity. V_{gly} was also significantly reduced in the FC group ($18.8 \pm 8.6 \text{ nmol} \cdot \text{g}^{-1} \cdot \text{min}^{-1}$) versus the LC group (56.2 ± 16.6 , $P < 0.02$) but was normalized in the FRSG group ($52.9 \pm 9.1 \text{ nmol} \cdot \text{g}^{-1} \cdot \text{min}^{-1}$, $P < 0.02$ vs. FC, Table 1). Therefore, the decreased glucose disposal observed in the FC group was associated with an ~78% reduction in glycogen synthesis flux and an ~67% reduction in V_{gly} , whereas these fluxes in the FRSG group were normalized to the LC group. Although muscle glycogen synthesis and glycolysis fluxes are normalized after rosiglitazone treatment, whole-body GDR is only partially normalized.

In vivo ^{31}P NMR. Figure 5A illustrates a ^{31}P NMR baseline spectrum with G-6-P (part of the phosphomonoester region), inorganic phosphate (both extracellular and intracellular), PCr (assigned to 0 ppm), and α -, β -, and γ -ATP indicated. The basal G-6-P concentrations were the same in all groups before the euglycemic-hyperinsulinemic clamp (165 ± 12 , 152 ± 29 , and $147 \pm 29 \text{ nmol/g}$ in the LC, FRSG, and FC groups, respectively; Fig. 5B). At 150 min, [G-6-P] increased in both the LC and FRSG groups ($16.9 \pm 5.8\%$ and $13.0 \pm 11.1\%$ vs. baseline, respectively) but decreased in the FC group ($-23.3 \pm 13.4\%$ vs. baseline, $P < 0.05$ vs. LC and FRSG groups, Fig. 5B).

Intramyocellular glucose. There were no differences in intramyocellular glucose after correction for intra-/extracellular glucose space (0.88 ± 0.32 , 0.38 ± 0.18 , and $0.48 \pm 0.26 \text{ mmol/l}$ in LC, FRSG, and FC groups, respectively).

DISCUSSION

The data reported here show that after 7-day rosiglitazone treatment in the Zucker fatty rat, insulin-stimulated whole-body glucose disposal was increased and muscle glycogen synthesis and glycolysis were normalized. Although TZDs, including rosiglitazone, have been shown to improve glycemic control in animal models of type 2 diabetes by reducing insulin resistance in muscle (1,3,4), liver (1,4), and adipose tissue (5,6), in vivo characterization of the glucose metabolic fate in these tissues has been difficult to achieve. In the present study, an in vivo NMR spectroscopic technique was used to noninvasively measure insulin-stimulated glucose disposal in the hindlimb muscles of an awake rat.

Using in vivo ^{13}C NMR spectroscopy, glycogen synthesis was shown to be increased in skeletal muscle of either type 2 diabetic (12) or insulin-resistant obese (30) subjects treated with troglitazone. Although whole-body glucose oxidation as measured by indirect calorimetry was increased in the troglitazone-treated type 2 diabetic subjects, the skeletal muscle V_{gly} was not ascertained (12). The direct in vivo effect of acute troglitazone stimulation on glycolysis was measured in perfused Sprague-Dawley rat hindlimb (31). The investigators showed that in the presence of troglitazone alone (no exogenous insulin), O_2 consumption and lactate/pyruvate release were increased with no exogenous fatty acids present in the perfusate.

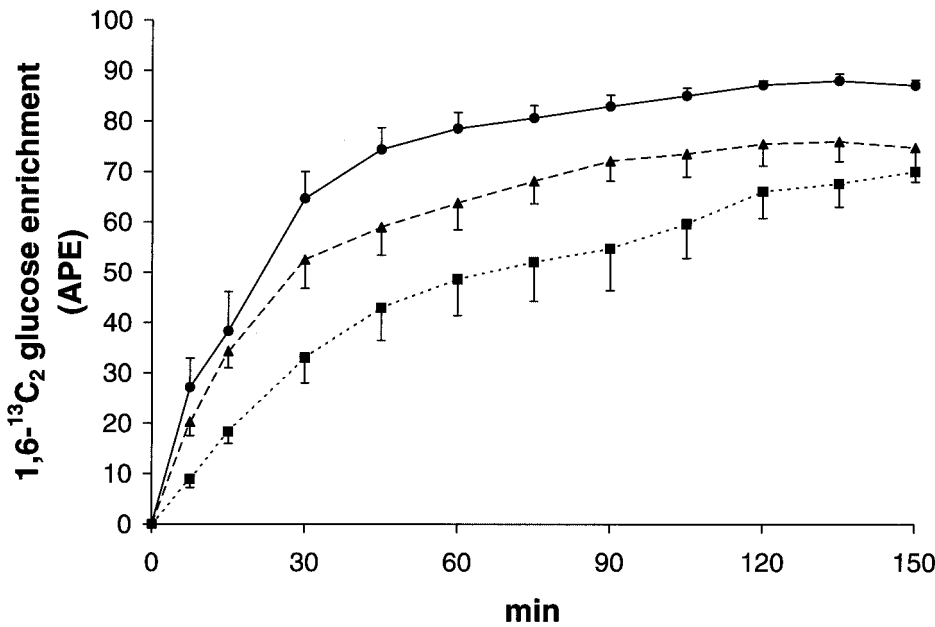


FIG. 2. 1,6-¹³C₂ glucose enrichment turnover kinetics during the euglycemic-hyperinsulinemic clamp. Absolute 1,6-¹³C₂ glucose (APE) in the LC (●), FRSG (▲), and FC (■) groups during a steady-state euglycemic-hyperinsulinemic clamp is shown. Data are means ± SE.

Therefore, it was postulated that both aerobic and nonaerobic glycolysis was stimulated by the TZD. However, these hindlimb perfusion experiments were not performed in chronically TZD-treated or insulin-resistant animal models.

The necessity for an *in vivo* noninvasive measurement of both glycogen synthesis and glycolysis becomes increasingly apparent in the presence of differing results with regard to the glucose metabolic fate as measured in isolated muscle strips after *in vitro* TZD incubation (32,33) or chronic oral TZD treatment (34–37). Fürsinn et al. (32) showed that *in vitro* troglitazone incubation elicited a glucose catabolic response in excised Sprague-Dawley soleus muscle strips. Using U-¹⁴C glucose tracer techniques for flux measurements, both glycogen synthesis

and glucose oxidation were decreased after insulin administration, whereas anaerobic glycolysis (measured as lactate release) increased to the extent that the anaerobic/aerobic glycolysis ratio was ~50:1. However, these data contrast with a number of studies that have examined the *in vivo* effects of chronic oral TZD treatment on skeletal muscle glucose metabolism (glycogen synthesis and glycolysis) in insulin-resistant rodent models (34–37). Although direct *in vivo* measurements of these fluxes were not performed, these studies nevertheless show that TZDs can act by various degrees to normalize both glycogen synthesis and glycolysis. After 4-day englitazone treatment in *ob/ob* mice, both insulin-stimulated glycogen synthesis and glycolysis were normalized, as assessed in incubated soleus muscle strips using 1-¹⁴C glucose to measure gly-

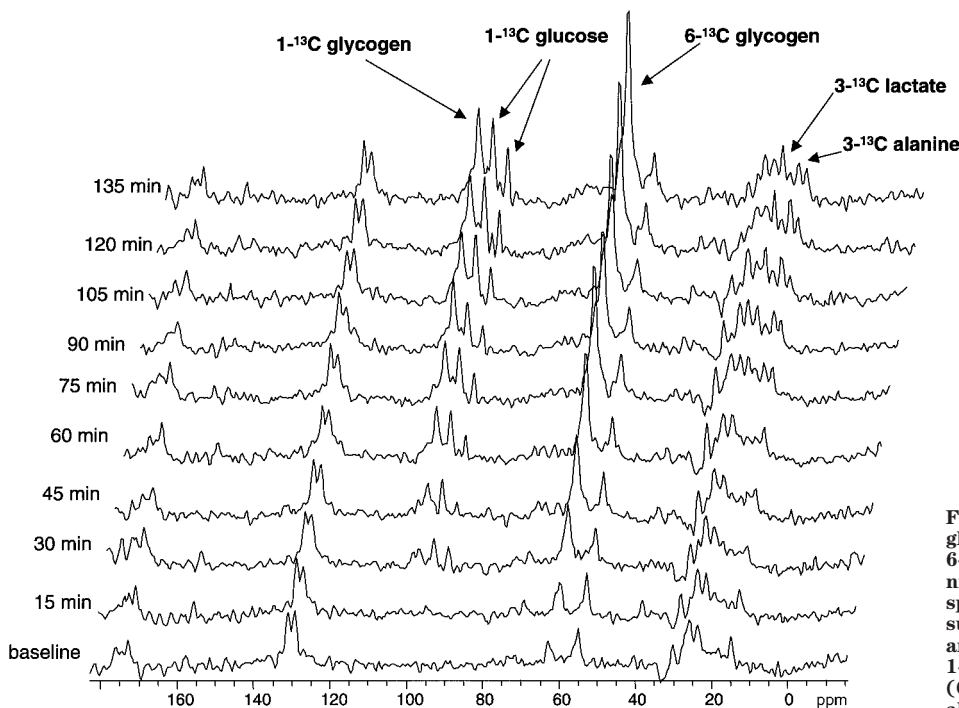


FIG. 3. *In vivo* ¹³C NMR spectra of 1,6-¹³C₂ glucose label incorporation into 1-¹³C and 6-¹³C glycogen, 3-¹³C lactate, and 3-¹³C alanine. A series of 15-min baseline subtracted spectra acquired during a euglycemic-hyperinsulinemic clamp are shown. 1-¹³C glucose (β-anomer, 96.8 ppm, and α-anomer, 93.0 ppm), 1-¹³C glycogen (100.5 ppm), 6-¹³C glycogen (61.4 ppm), 3-¹³C lactate (21.0 ppm), and 3-¹³C alanine (16.9 ppm) are visible where indicated.

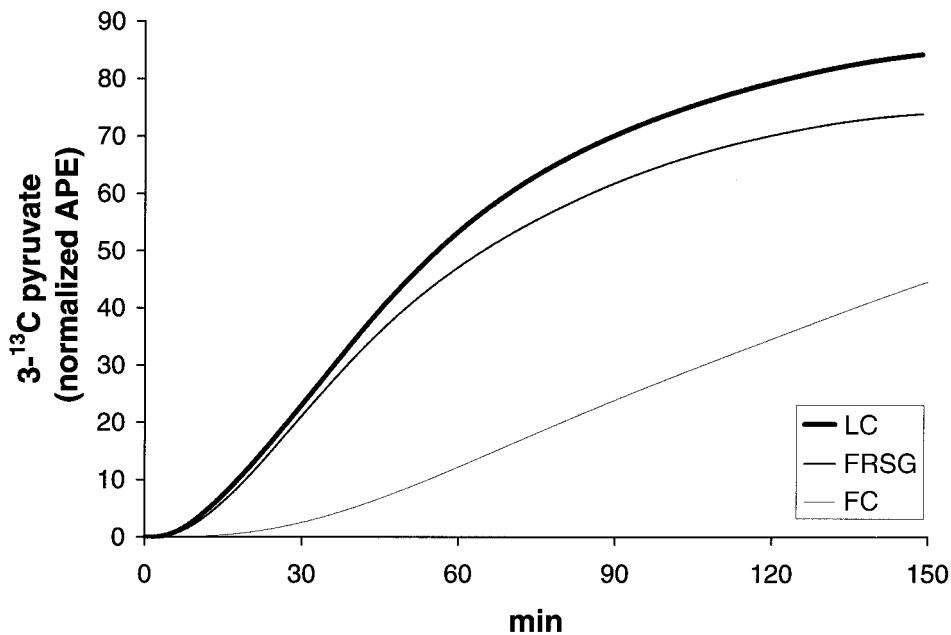


FIG. 4. Computer-fit $3\text{-}^{13}\text{C}$ pyruvate turnover curves to the NMR acquired $3\text{-}^{13}\text{C}$ lactate and $3\text{-}^{13}\text{C}$ alanine turnover data. The increased rate at which $3\text{-}^{13}\text{C}$ pyruvate turns over in the FRSG and LC groups versus the FC group may be used as a qualitative marker of increased flux through glycolysis in these groups. Absolute V_{gly} was calculated using a nonlinear least-squares fit of the experimental $3\text{-}^{13}\text{C}$ lactate and $3\text{-}^{13}\text{C}$ alanine turnover data to the model-generated $3\text{-}^{13}\text{C}$ pyruvate curve.

cogen synthesis and glucose oxidation and $3\text{-}^3\text{H}$ glucose to measure glycolysis (34). An interesting result of this study was that basal glucose oxidation was increased after

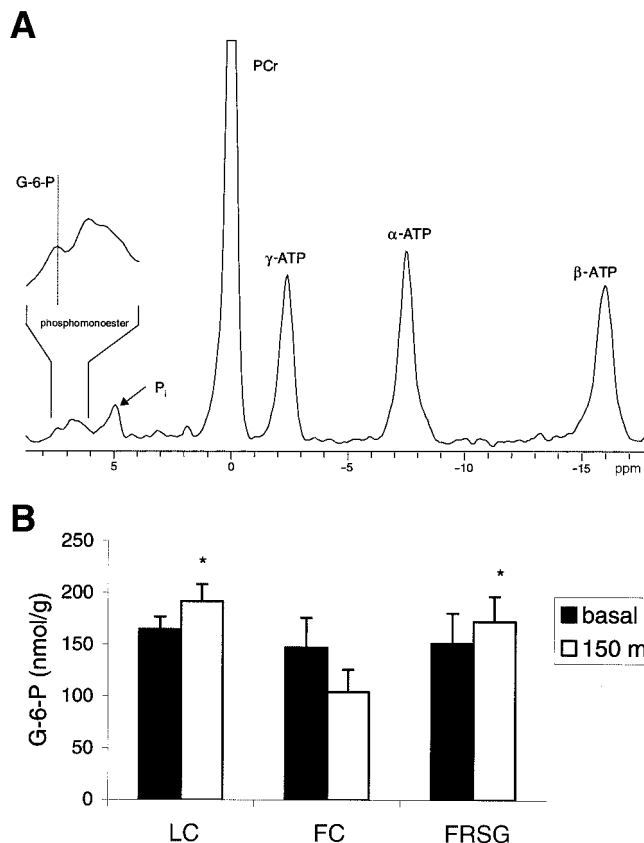


FIG. 5. ^{31}P NMR spectrum and G-6-P kinetics. A: A 10-min-acquired ^{31}P NMR baseline spectrum with G-6-P (in the phosphomonoester region [see zoomed in area]), inorganic phosphate (P_i) (both extracellular and intracellular), PCr (assigned to 0 ppm), and α -, β -, and γ -ATP is indicated. B: The basal [G-6-P] was the same in all groups before the euglycemic-hyperinsulinemic clamp. At 150 min, [G-6-P] increased in both the LC and FRSG groups but decreased in the FC group ($P < 0.05$ vs. LC and FRSG groups). * $P < 0.05$ vs. FC at 150 min.

englitazone treatment and normalized to the lean group. More recently, Sreenan et al. (35) showed that the increased insulin-stimulated glucose disposal, as measured using 2-deoxyglucose in 6-week troglitazone-treated ZDF rat soleus muscle, was also due to an increase in both glycogen synthesis and glycolysis. Also of note was that troglitazone almost doubled the basal glucose oxidation flux in these rats. This result correlated with an enhancement of muscle pyruvate dehydrogenase activity under basal conditions in the study. Fürnsinn et al. (36) examined the effects of treatment with the TZDs BM13.1258 and BM15.2054 on glucose intermediary metabolism. In this study, insulin-stimulated glycogen synthesis, as measured in isolated soleus, was increased after 10-day oral treatment of either TZD in Zucker fatty rats, yet glucose transport and oxidation was only increased in the BM13.1258-treated rats. These results suggest that different TZDs exhibit different responses with regard to glycogen synthesis and glucose oxidation and therefore may control glucose metabolism via multiple mechanisms.

Further to the notion that TZDs may exhibit control of glucose disposal through multiple mechanisms is that TZDs appear not to exhibit the same degree of insulin sensitivity in all tissue. Although both glycogen synthesis and glucose metabolism in hindlimb skeletal muscle of Zucker fatty rats were normalized after 7-day rosiglitazone treatment in the present study, whole-body GDR was only partially normalized (73% of control). This discrepancy is most likely due to a noneffect of rosiglitazone on insulin-stimulated glucose disposal in other tissue (e.g., heart and adipose tissue) (1).

Measurements of [G-6-P] along with glycogen synthesis and V_{gly} can be used to provide an index of metabolic control (12). For example, as insulin stimulated hexokinase and glycogen synthase in the FC group, glucose transport could not keep up with the demand, which resulted in a decrease in [G-6-P] versus the LC and FRSG groups. This hypothesis holds true if intracellular glucose were held constant or lower in the FC versus the LC and

FRSG groups. Although there were no significant differences between the groups, there was large variability in our intracellular glucose measurement. Therefore, it is difficult to delineate the role of glucose transport versus hexokinase in the control of glucose uptake in this model. Although there is as yet no direct evidence for an effect of rosiglitazone on GLUT4 expression or function in skeletal muscle, rosiglitazone corrects expression levels of the skeletal muscle proteins cellubrevin, VAMP-2, and syntaxin-4, which are known to be associated with GLUT4 vesicle trafficking in skeletal muscle of hyperglycemic ZDF rats (38).

In summary, a combined in vivo ^{13}C and ^{31}P NMR spectroscopic approach was used to measure skeletal muscle glucose uptake and its distributed fluxes (glycogen synthesis and glycolysis) and G-6-P (a key metabolic intermediate) during a euglycemic-hyperinsulinemic clamp in awake Zucker fatty rats. The data suggest that the increased insulin-stimulated glucose disposal in skeletal muscle associated with rosiglitazone treatment was attributed to a normalization of both glycogen synthesis and glycolysis.

ACKNOWLEDGMENTS

We are indebted to Kimberly Brown, Diane McGee, and Kathleen Morasco for their expert technical assistance. We are also grateful to Peter Brown, Yale University School of Medicine, for radio frequency antenna design and construction.

REFERENCES

- Oakes ND, Kennedy CJ, Jenkins AB, Laybutt DR, Chisholm DJ, Kraegen EW: A new antidiabetic agent, BRL 49653, reduces lipid availability and improves insulin action and glucoregulation in the rat. *Diabetes* 43:1203-1210, 1994
- Young PW, Cawthorne MA, Coyle PJ, Holder JC, Holman GD, Kozka IJ, Kirkham DM, Lister CA, Smith SA: Repeat treatment of obese mice with BRL 49653, a new potent insulin sensitizer, enhances insulin action in white adipocytes: association with increased insulin binding and cell-surface GLUT4 as measured by photoaffinity labeling. *Diabetes* 44:1087-1092, 1995
- Eldershaw TP, Rattigan S, Cawthorne MA, Buckingham RE, Colquhoun EQ, Clark MG: Treatment with the thiazolidinedione (BRL 49653) decreases insulin resistance in obese Zucker hindlimb. *Horm Metab Res* 27:169-172, 1995
- Oakes ND, Camilleri S, Furler SM, Chisholm DJ, Kraegen EW: The insulin sensitizer, BRL 49653, reduces systemic fatty acid supply and utilization and tissue lipid availability in the rat. *Metabolism* 46:935-942, 1997
- Kanoh Y, Bandyopadhyay G, Sajan MP, Standaert ML, Farese RV: Rosiglitazone, insulin treatment, and fasting correct defective activation of protein kinase C-zeta/lambd by insulin in vastus lateralis muscles and adipocytes of diabetic rats. *Endocrinology* 142:1595-1605, 2001
- Young PW, Buckle DR, Cantello BC, Chapman H, Clapham JC, Coyle PJ, Haigh D, Hindley RM, Holder JC, Kallender H, Latter AJ, Lawrie KW, Mossakowska D, Murphy GJ, Roxbee Cox L, Smith SA: Identification of high-affinity binding sites for the insulin sensitizer rosiglitazone (BRL-49653) in rodent and human adipocytes using a radiolabeled ligand for peroxisomal proliferator-activated receptor gamma. *J Pharmacol Exp Ther* 284:751-759, 1998
- DeFronzo RA, Jacot E, Jequier E, Maeder E, Wahren J, Felber JP: The effect of insulin on the disposal of intravenous glucose: results from indirect calorimetry and hepatic and femoral venous catheterization. *Diabetes* 30:1000-1007, 1981
- Hevener AL, Reichart D, Olefsky J: Exercise and thiazolidinedione therapy normalize insulin action in the obese Zucker fatty rat. *Diabetes* 49:2154-2159, 2000
- Park KS, Ciaraldi TP, Abrams-Carter L, Mudaliar S, Nikolouina SE, Henry RR: Troglitazone regulation of glucose metabolism in human skeletal muscle cultures from obese type II diabetic subjects. *J Clin Endocrinol Metab* 83:1636-1643, 1998
- Zierath JR, Ryder JW, Doebber T, Woods J, Wu M, Ventre J, Li Z, McCrory C, Berger J, Zhang B, Moller DE: Role of skeletal muscle in thiazolidinedione insulin sensitizer (PPARgamma agonist) action. *Endocrinology* 139:5034-5041, 1998
- Hallakou S, Fougelle F, Doare L, Kergoat M, Ferre P: Pioglitazone-induced increase of insulin sensitivity in the muscles of the obese Zucker fa/fa rat cannot be explained by local adipocyte differentiation. *Diabetologia* 41:963-968, 1998
- Petersen KF, Krssak M, Inzucchi S, Cline GW, Dufour S, Shulman GI: Mechanism of troglitazone action in type 2 diabetes. *Diabetes* 49:827-831, 2000
- Schoonjans K, Staels B, Auwerx J: The peroxisome proliferator activated receptors (PPARs) and their effects on lipid metabolism and adipocyte differentiation. *Biochim Biophys Acta* 1302:93-109, 1996
- Yonemitsu S, Nishimura H, Shintani M, Inoue R, Yamamoto Y, Masuzaki H, Ogawa Y, Hosoda K, Inoue G, Hayashi T, Nakao K: Troglitazone induces GLUT4 translocation in L6 myotubes. *Diabetes* 50:1093-1101, 2001
- Oakes ND, Thalen PG, Jacinto SM, Ljung B: Thiazolidinediones increase plasma-adipose tissue FFA exchange capacity and enhance insulin-mediated control of systemic FFA availability. *Diabetes* 50:1158-1165, 2001
- Krssak M, Falk Petersen K, Dresner A, DiPietro L, Vogel SM, Rothman DL, Roden M, Shulman GI: Intramyocellular lipid concentrations are correlated with insulin sensitivity in humans: a ^1H NMR spectroscopy study. *Diabetologia* 42:113-116, 1999
- Jacob S, Machann J, Rett K, Brechtel K, Volk A, Renn W, Maerker E, Matthaei S, Schick F, Claussen CD, Haring HU: Association of increased intramyocellular lipid content with insulin resistance in lean nondiabetic offspring of type 2 diabetic subjects. *Diabetes* 48:1113-1119, 1999
- Virkkamaki A, Korshennikova E, Seppala-Lindroos A, Vehkavaara S, Goto T, Halavaara J, Hakkinen AM, Yki-Jarvinen H: Intramyocellular lipid is associated with resistance to in vivo insulin actions on glucose uptake, antilipolysis, and early insulin signaling pathways in human skeletal muscle. *Diabetes* 50:2337-2343, 2001
- Dresner A, Laurent D, Marcucci M, Griffin ME, Dufour S, Cline GW, Slezak LA, Andersen DK, Hundal RS, Rothman DL, Petersen KF, Shulman GI: Effects of free fatty acids on glucose transport and IRS-1-associated phosphatidylinositol 3-kinase activity. *J Clin Invest* 103:253-259, 1999
- Griffin ME, Marcucci MJ, Cline GW, Bell K, Barucci N, Lee D, Goodyear LJ, Kraegen EW, White MF, Shulman GI: Free fatty acid-induced insulin resistance is associated with activation of protein kinase C theta and alterations in the insulin signaling cascade. *Diabetes* 48:1270-1274, 1999
- Jucker BM, Rennings AJM, Cline GW, Shulman GI: ^{13}C and ^{31}P NMR studies on the effects of increased plasma free fatty acids on intramuscular glucose metabolism in the awake rat. *J Biol Chem* 272:10464-10473, 1997
- Smith D, Rossetti L, Ferrannini E, Johnson CM, Cobelli C, Toffolo G, Katz LD, DeFronzo RA: In vivo glucose metabolism in the awake rat: tracer and insulin clamp studies. *Metabolism* 36:1176-1186, 1987
- McIntosh TS, Davis HM, Matthews DE: A liquid chromatography-mass spectrometry method to measure stable isotopic tracer enrichments of glycerol and glucose in human serum. *Analytical Biochem* 300:163-169, 2002
- Kepler D, Decker K: *Methods of Enzymatic Analysis*. Bergmeyer HU, Ed. New York, Verlag Chemie Weinheim, Academic Press, 1974, p. 1127-1131
- Cline GW, Jucker BM, Trajanoski Z, Rennings AJ, Shulman GI: A novel ^{13}C NMR method to assess intracellular glucose concentration in muscle, in vivo. *Am J Physiol Endocrinol Metab* 274:E381-E389, 1998
- Bloch G, Chase JR, Meyer DB, Avison MJ, Shulman GI, Shulman RG: In vivo regulation of rat muscle glycogen resynthesis after intense exercise. *Am J Physiol Endocrinol Metab* 266:E85-E91, 1994
- Jucker BM, Rennings AJM, Cline GW, Petersen KF, Shulman GI: In vivo NMR investigation of intramuscular glucose metabolism in conscious rats. *Am J Physiol Endocrinol Metab* 273:E139-E148, 1997
- Rossetti L, Giaccari A: Relative contribution of glycogen synthesis and glycolysis to insulin-mediated glucose uptake. *J Clin Invest* 85:1785-1792, 1990
- Kim JK, Wi JK, Youn JH: Plasma free fatty acids decrease insulin-stimulated skeletal muscle glucose uptake by suppressing glycolysis in conscious rats. *Diabetes* 45:446-453, 1996
- Van Den Bergh AJ, Tack CJ, Van Den Boogert HJ, Vervoort G, Smits P, Heerschap A: Assessment of human muscle glycogen synthesis and total glucose content by in vivo ^{13}C MRS. *Eur J Clin Invest* 30:122-128, 2000
- Okuno A, Ikeda K, Shiota M, Fujiwara T, Yoshioka S, Sugano T, Horikoshi H: Acute effect of troglitazone on glucose metabolism in the absence or presence of insulin in perfused rat hindlimb. *Metabolism* 46:716-721, 1997

32. Fürsinn C, Neschen S, Noe C, Bisschop M, Roden M, Vogl C, Schneider B, Waldhausl W: Acute non-insulin-like stimulation of rat muscle glucose metabolism by troglitazone *in vitro*. *Br J Pharmacol* 122:1367–1374, 1997
33. Fürsinn C, Brunmair B, Neschen S, Roden M, Waldhausl W: Troglitazone directly inhibits CO₂ production from glucose and palmitate in isolated rat skeletal muscle. *J Pharmacol Exp Ther* 293:487–493, 2000
34. Stevenson RW, Hutson NJ, Krupp MN, Volkmann RA, Holland GF, Eggler JF, Clark DA, McPherson RK, Hall KL, Danbury BH, Gibbs EM, Kreutter DK: Actions of novel antidiabetic agent englitazone in hyperglycemic hyperinsulinemic ob/ob mice. *Diabetes* 39:1218–1227, 1990
35. Sreenan S, Keck S, Fuller T, Cockburn B, Burant CF: Effects of troglitazone on substrate storage and utilization in insulin-resistant rats. *Am J Physiol* 276:E1119–E1129, 1999
36. Fürsinn C, Brunmair B, Meyer M, Neschen S, Furtmüller R, Roden M, Kuhnle HF, Nowotny P, Schneider B, Waldhausl W: Chronic and acute effects of thiazolidinediones BM13.1258 and BM15.2054 on rat skeletal muscle glucose metabolism. *Br J Pharmacol* 128:1141–1148, 1999
37. Sugiyama Y, Taketomi S, Shimura Y, Ikeda H, Fujita T: Effects of pioglitazone on glucose and lipid metabolism in Wistar fatty rats. *Arzneimittelforschung* 40:263–267, 1990
38. Maier VH, Melvin DR, Lister CA, Chapman H, Gould GW, Murphy GJ: v- and t-SNARE protein expression in models of insulin resistance: normalization of glycemia by rosiglitazone treatment corrects overexpression of cellubrevin, vesicle-associated membrane protein-2, and syntaxin 4 in skeletal muscle of Zucker diabetic fatty rats. *Diabetes* 49:618–625, 2000